

Scalable Exact Verification of Optimization Proxies for Large-Scale Optimal Power Flow

Rahul Nellikkath
Spyros Chatzivasileiadis
Denmark Technical University
{rnelli,spchatz}@dtu.dk

Mathieu Tanneau
Pascal Van Hentenryck
Georgia Institute of Technology
{mathieu.tanneau, pascal.vanhentenryck}@isye.gatech.edu

Abstract—Optimal Power Flow (OPF) is a valuable tool for power system operators, but it is a difficult problem to solve for large systems. Machine Learning (ML) algorithms, especially Neural Networks-based (NN) optimization proxies, have emerged as a promising new tool for solving OPF, by estimating the OPF solution much faster than traditional methods. However, these ML algorithms act as black boxes, and it is hard to assess their worst-case performance across the entire range of possible inputs than an OPF can have. Previous work has proposed a mixed-integer programming-based methodology to quantify the worst-case violations caused by a NN trained to estimate the OPF solution, throughout the entire input domain. This approach, however, does not scale well to large power systems and more complex NN models. This paper addresses these issues by proposing a scalable algorithm to compute worst-case violations of NN proxies used for approximating large power systems within a reasonable time limit. This will help build trust in ML models to be deployed in large industry-scale power grids.

Index Terms—Optimal Power Flow, Neural Networks, Trustworthy Machine Learning, Worst-Case Guarantees.

I. INTRODUCTION

The Optimal Power Flow (OPF) problem [1] is a fundamental problem in power systems operations. It is routinely used for clearing day-ahead and real-time electricity markets, for planning, to compute optimal control setpoints, and to conduct reliability analyses. However, in its original form, the AC-OPF problem is often challenging to solve as it is a non-linear and non-convex optimization. Recent years have witnessed a surge of interest in optimization proxies for OPF, i.e., Machine Learning (ML) models that approximate the input/output mapping of OPF [2] [3], [4], [5]. Once trained, optimization proxies can produce high-quality, close-to-feasible solutions to OPF in milliseconds, thereby overcoming the computational barrier of AC-OPF for large, industry-scale power grids. Additionally, trained ML models have shown great potential in serving as fast surrogate functions to replace computationally intensive constraints [6] or bi-level optimization problems.

Nevertheless, the black-box nature of optimization proxies poses a significant challenge to their deployment and adoption

in industry. In general, optimization proxies come without formal guarantees across the entire range of possible inputs, which is particularly concerning considering the potential use of OPF in safety-critical applications. This has motivated the use of Neural Network (NN) verification to quantify an optimization proxy’s worst-case performance [7].

State-of-the-art approaches for NN verification first build a mixed-integer programming (MIP) representation of the NN, then solve a MIP problem to provably compute its worst-case performance across a given input domain [7], [8], [9]. Prior works have demonstrated how various worst-case guarantees can be computed for DC-OPF [7], [8] and AC-OPF problems [9], [10]. Furthermore, prior research has demonstrated how to use NN verification and worst-case guarantees to build a trustworthy NN [11], [12].

While existing verification approaches leverage mature MIP technology, their high computational cost has so far limited their applications to small power grids and simple NN models. This research is a step in addressing this limitation. It proposes new primal and dual acceleration techniques to improve the scalability of OPF proxies verification and demonstrates their performance on large power grids. More precisely, the paper makes three contributions:

- 1) The paper shows how to find adversarial test cases quickly, by using gradient-based strategies that exploit the structure of OPF problems. These test cases can then be used to warm-start the verification MIP and obtain better primal bounds faster.
- 2) The paper shows the benefits of advanced bound-tightening techniques and, in particular, α, β -CROWN [13], [14], [15], [16] to tighten the MIP dual bounds. Again, these techniques leverage the properties of OPF problems to reduce the complexity of the MIP problem and help the dual bound converge faster.
- 3) The paper shows that these acceleration techniques makes it possible to formally verify OPF proxies for large power grids that are an order of magnitude larger than those used in existing approaches.

This rest of the paper is structured as follows. Section II describes the DC-OPF [17] problem and the optimization algorithm used to determine the worst-case guarantees. Section III introduces the proposed methods for accelerating the NN

This research was partly supported by NSF award 2112533 and by the ERC Starting Grant VeriPhIED, funded by the European Research Council, Grant Agreement 949899.



Model 1 The DC-OPF Model

$$\min c^\top \mathbf{p}^g \quad (1a)$$

$$\text{s.t. } \mathbf{e}^\top \mathbf{p}^g = \mathbf{e}^\top \mathbf{p}^d \quad (1b)$$

$$\underline{\mathbf{p}}^g \leq \mathbf{p}^g \leq \overline{\mathbf{p}}^g \quad (1c)$$

$$|\Phi(\mathbf{p}^g - \mathbf{p}^d)| \leq \overline{\mathbf{p}}^f \quad (1d)$$

verification. Section IV provides the simulation setup used and reports the results demonstrating the performance of proposed techniques. Section V discusses the possible opportunities to further improve the system performance and draw the conclusions of the paper.

II. DNN VERIFICATION FOR OPF PROXIES

The paper proposes new acceleration techniques to address existing scalability challenges in verifying OPF proxies, both on the primal and dual sides. The methodology is evaluated on DC-OPF proxies but, ultimately, similar approaches can be applied to verify AC-OPF proxies. In the following, the set of buses is denoted by $\mathcal{N} = \{1, \dots, N\}$ and the set of branches by $\mathcal{E} = \{1, \dots, E\}$. The vector of all ones is denoted by $\mathbf{e} = (1, \dots, 1)$. For ease of reading and without loss of generality, the presentation assumes that one generator and one load are attached to each bus, and that the costs are linear. Unless specified otherwise, all quantities are in per-unit (p.u.).

A. DC Optimal Power Flow

The DC optimal power flow (DC-OPF) is a linear approximation of AC-OPF, where voltage magnitudes are assumed to be 1p.u. and voltage angles are assumed to be small, losses are neglected, reactive power is ignored, and the power flow equations are linearized. The DC-OPF model underlies most electricity markets in the US.

Model 1 presents the DC-OPF linear programming (LP) model. The model takes, as inputs, the cost c , the demand \mathbf{p}^d , the lower and upper generation limits $\underline{\mathbf{p}}^g, \overline{\mathbf{p}}^g$, the Power Transfer Distribution Factor (PTDF) matrix $\Phi \in \mathbb{R}^{E \times N}$, and the thermal limits $\overline{\mathbf{p}}^f$. Its variables are the generation dispatches, which are denoted by \mathbf{p}^g . The objective (1a) minimizes the cost of generation. Constraint (1b) enforces the power balance in the system, i.e., total generation equals total demand. Constraints (1c) enforce minimum and maximum limits on generation dispatch. Constraints (1d) enforce thermal constraints on each branch.

B. Neural Networks for Optimal Power Flow Approximation

Neural networks (NNs) are universal function approximators. Given sufficient size and appropriate training, they can approximate any function, including the mapping between power system demand and the DC-OPF generation setpoints. This makes them a popular architecture for optimization proxies. NNs are comprised of a set of interconnected hidden layers with multiple neurons in each layer. Each neuron in a hidden layer receives inputs from the neurons in the previous layer

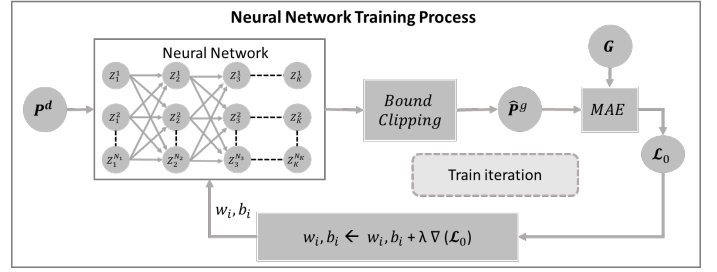


Fig. 1. Illustration of the neural network architecture to predict the optimal generation active power outputs $\hat{\mathbf{p}}^g$ using the active power demand \mathbf{p}^d as input: There are K hidden layers in the neural network with N_k neurons each. Where $k = 1, \dots, K$.

and applies a linear transformation to them. The output of this transformation is then passed through a nonlinear activation function. The activation function introduces nonlinearity into the network, which allows it to approximate a wider range of functions. The final layer of the NN outputs the predicted DC-OPF generation setpoints. The NN is trained by minimizing the error between the predicted and actual generation setpoints. For a NN with K hidden layers and N_k number of neurons in hidden layer k , as shown in fig. 1, the information arriving at layer k can be formulated as follows:

$$\hat{\mathbf{Z}}_k = \mathbf{w}_k \mathbf{Z}_{k-1} + \mathbf{b}_k \quad (2)$$

where \mathbf{Z}_{k-1} is the output of the neurons in layer $k-1$, $\hat{\mathbf{Z}}_k$ is the information received at layer k , \mathbf{w}_k and \mathbf{b}_k are the weights and biases connecting layer $k-1$ and k .

Each neuron in a NN applies a nonlinear activation function, e.g., the sigmoid function. The output of each layer in the NN can be represented as follows:

$$\mathbf{Z}_k = \sigma(\hat{\mathbf{Z}}_k) \quad (3)$$

where σ is the nonlinear activation function. This paper uses the rectified linear unit (ReLU) as the activation function: it can be formulated as follows:

$$\mathbf{Z}_k = \max(\hat{\mathbf{Z}}_k, 0) \quad (4)$$

The ReLU is a simple but effective activation function that has been shown to accelerate the NN training. Furthermore, since ReLU is piecewise linear, it can be used to estimate worst-case guarantees and achieve exact verification.

Since active power generation is limited by generation capacities (1c), the output of the NN is clipped. The bound clipping process can be denoted as follows:

$$\hat{\mathbf{p}}^g = \min(\max(\hat{\mathbf{Z}}_K, \underline{\mathbf{p}}^g), \overline{\mathbf{p}}^g) \quad (5)$$

This can also be implemented using two ReLUs as follows:

$$\hat{\mathbf{p}}^g = (\overline{\mathbf{p}}^g - \sigma(\overline{\mathbf{p}}^g - (\underline{\mathbf{p}}^g + \sigma(\hat{\mathbf{Z}}_K - \underline{\mathbf{p}}^g)))) \quad (6)$$

Given a set of active power demands of a system, this paper trains NNs to determine the optimal active power setpoints of the DC-OPF problem, as a guiding application. The average

error in predicting the optimal generation setpoints in the training data set, denoted by \mathcal{L}_0 , is measured as

$$\mathcal{L}_0 = \frac{1}{N} \sum_{i=1}^N |\mathbf{p}_i^g - \hat{\mathbf{p}}_i^g| \quad (7)$$

where N is the number of training data points, and $\mathbf{p}_i^g, \hat{\mathbf{p}}_i^g$ are the ground truth (produced by an optimization solver) and predicted (by the DNN) generation dispatches, respectively.

The backpropagation algorithm modifies the weights \mathbf{w} and biases \mathbf{b} in every iteration of the neural network (NN) training to minimize the mean prediction error \mathcal{L}_0 of the generation setpoints in the training set. However, minimizing the mean error does not guarantee constraint compliance for all the input combinations in the input domain. Thus, verifying the NN performance and quantifying the worst-case guarantees is essential for deployment.

C. Worst-Case Guarantees for Neural Networks

The goal of the exact verification is to provide worst-case guarantees on the predictions of a NN. These worst-case guarantees provide an upper bound on constraint violations, which can be used to ensure that the NN will always produce “reasonable” setpoints, even under adversarial conditions.

To determine these worst-case guarantees, the trained NN is reformulated into a mixed-integer linear programming (MILP) problem using the method proposed in [7]. This involves converting the non-linear activation functions into linear constraints. The NN formulation given in Equation (2) is linear and can thus be used directly in the MILP formulation for verification. However, the non-linear ReLU activation (4) and the bound clipping must be reformulated to be integrated into the MILP-based verifier:

$$\mathbf{Z}_k = \max(\hat{\mathbf{Z}}_k, 0) \Rightarrow \begin{cases} \mathbf{Z}_k \leq \hat{\mathbf{Z}}_k - \underline{\mathbf{Z}}_k(1 - \mathbf{y}_k) & (8a) \\ \mathbf{Z}_k \geq \hat{\mathbf{Z}}_k & (8b) \\ \mathbf{Z}_k \leq \bar{\mathbf{Z}}_k \mathbf{y}_k & (8c) \\ \mathbf{Z}_k \geq \mathbf{0} & (8d) \\ \mathbf{y}_k \in \{0, 1\}^{N_k} & (8e) \end{cases}$$

where \mathbf{Z}_k and $\hat{\mathbf{Z}}_k$ are the outputs and inputs of the ReLU activation function, $\underline{\mathbf{Z}}_k$ and $\bar{\mathbf{Z}}_k$ are large big-M values whose bound constraints cannot be binding, and \mathbf{y}_k is the binary variable.

1) *Worst-Case Guarantees for Constraint Violations:* This section describes the MILP-based NN verifiers used to determine the maximum line flow constraint violations and the maximum power-flow imbalance as a result of the NN. The worst-case line flow constraint violation in line e can be determined by the MILP-based NN verifier:

$$v_e^l = \max_{\mathbf{p}^d} \max(0, |\mathbf{p}_e^f - \bar{\mathbf{p}}_e^f|) \quad (9a)$$

$$\text{s.t. } (2), (8a) - (8e) \quad (9b)$$

$$\mathbf{p}^f = \Phi(\hat{\mathbf{p}}^g - \mathbf{p}^d) \quad (9c)$$

$$\underline{\mathbf{p}}^d \leq \mathbf{p}^d \leq \bar{\mathbf{p}}^d \quad (9d)$$

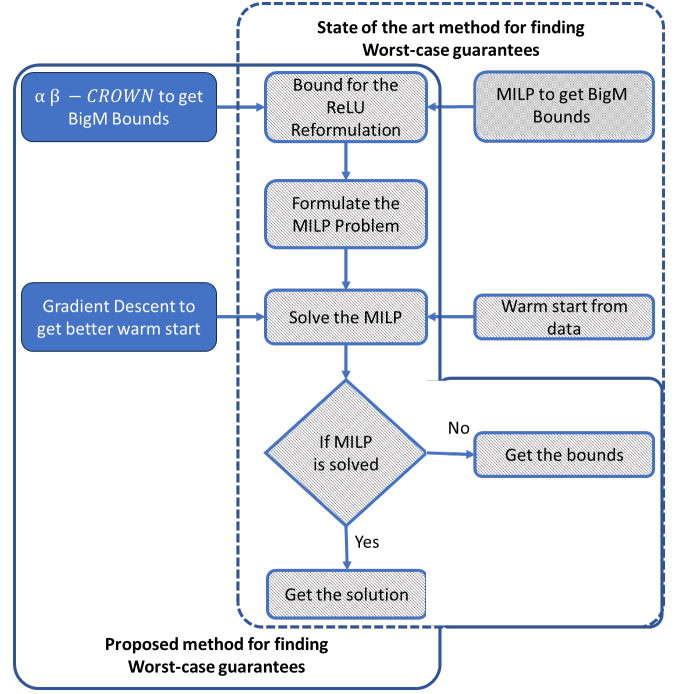


Fig. 2. Proposed Method for accelerating the NN exact verification for computing worst-case guarantees

The worst-case violation across all lines is then $v^l = \max_{e \in \mathcal{E}} (v_e^l)$. The worst-case power balance violation can be formulated similarly:

$$v^{\text{PB}} = \max_{\mathbf{p}^d} |\mathbf{e}^\top \mathbf{p}^d - \mathbf{e}^\top \hat{\mathbf{p}}^g| \quad (10a)$$

$$\text{s.t. } (2), (8a) - (8e) \quad (10b)$$

$$\underline{\mathbf{p}}^d \leq \mathbf{p}^d \leq \bar{\mathbf{p}}^d \quad (10c)$$

Solving these MILP-based NN verifiers to optimality ensures that the v^l and v^{PB} values so obtained are global optima. As a result, they guarantee that there is no input \mathbf{p}^d in the entire input domain leading to constraint violations larger than the obtained values.

III. ACCELERATION TECHNIQUES

The strength of the MIP formulation directly impacts the quality of the worst-case guarantees. Weak MIP formulations require significant –and costly– branching to close the gap between primal and dual bounds. This paper proposes two methods for accelerating the solving of MILP verifiers that computes worst-case guarantees for NNs. The overall methodology is presented in fig. 2, which also contrasts the proposed and prior approaches.

There are two innovations in the proposed approaches, addressing dual and primal bounds of the MILP-based NN verifiers respectively. The first innovation is the use of advanced branch and bound algorithms used for NN verification, in particular, α, β -CROWN [13], [14], [15], [16] for optimization-based bounds tightening (OBBT) to obtain tighter big-M bounds for the ReLU relaxations. Using better big-M bounds tightens the MILP relaxation and improves the dual bound.

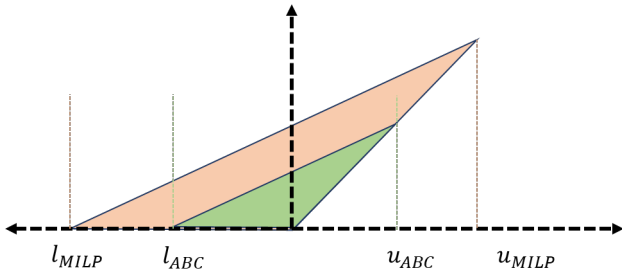


Fig. 3. Illustrates the feasible region for Relaxed ReLU. Here $y = \text{ReLU}(X)$. A tighter bound for the ReLU results in a tighter relaxation.

The second innovation concerns primal bounds: it aims at finding strong primal solutions that can be used to warm-start the MILP-based verifier. The proposed methodology uses gradient descent to quickly find these primal solutions, which may dramatically improve the convergence speed of the MILP solver. Indeed, the MILP-based verifiers face challenges both in finding strong primal and dual bounds.

The authors also implemented general cutting planes from [18] to further tighten the linear relaxation of the MILP-based verifier. These cuts were found ineffective, sometimes even degrading performance on the larger grids. These results are thus omitted due to space considerations.

A. α, β -CROWN for Tighter Big-M Bounds

The big-M reformulations of ReLU neurons, shown in equations (8a)–(8e), replace the ReLU activation function with a mixed integer function bounded above and below. For the MILP algorithm to converge, the primal bound, which satisfies all the constraints, including the binary variable constraints, must equal the dual bound, a relaxed linear problem with some of the binary variables defined as continuous variables $\in [0, 1]$. Tighter and more accurate upper and lower bounds for the ReLU function result in a tighter feasible region for the relaxed MILP problem, as shown in fig. 3, thus resulting in a tighter dual bound.

Prior work on bound tightening for ReLU used interval bound propagation (IBP) and MILP-based tightening. IBP bounds are commonly used to find the upper and lower bounds of the ReLU function for NN verification: they can be computed relatively quickly, but are usually loose, especially as the depth of the network increases. MILP-based tightening [7] has been proposed as an alternative to IBP for bound tightening. MILP-based tightening must solve two MILPs for finding the big-M bound at each node: one to find the lower bound and one to find the upper bound. The MILP problem for finding the lower bound can be formulated as follows:

$$\underline{z}_k = \min_{\mathbf{p}^d} \hat{\mathbf{z}}_k \quad (11a)$$

$$\text{s.t. } (2), (8a) - (8e) \quad (11b)$$

$$\underline{\mathbf{p}}^d \leq \mathbf{p}^d \leq \bar{\mathbf{p}}^d \quad (11c)$$

Similarly, the MILP problem for finding the upper bound can be formulated as follows:

$$\bar{z}_k = \max_{\mathbf{p}^d} \hat{\mathbf{z}}_k \quad (12a)$$

$$\text{s.t. } (2), (8a) - (8e) \quad (12b)$$

$$\underline{\mathbf{p}}^d \leq \mathbf{p}^d \leq \bar{\mathbf{p}}^d \quad (12c)$$

These MILPs must not be solved to optimality: instead, they may be run for a few seconds, and the obtained bounds can be used as the big-M values. Furthermore, this is a highly parallelizable task. However, the MILP-based tightening is also a computationally intensive task for large power systems.

As an alternative, this paper proposes the use of one of the top branch and bound algorithms in the NN verification competitions [19]: α, β -CROWN proposed in [13], [15] to achieve tighter big-M bounds. α, β -CROWN is a fast and scalable NN verifier that uses an efficient linear bound propagation, branch and bound procedure, and GPU acceleration to find better bounds. Similar to the MILP method proposed in [7], α, β -CROWN must be run twice, once to get the upper bound, denoted by u_{ABC} , and the lower bound, denoted by l_{ABC} , per ReLU. However, similar to the MILP method for bound tightening, the verification can be parallelized on GPUs.

B. Gradient Descent for Strong Primal Solutions

As mentioned earlier, on the primal side, general-purpose MIP solvers also fail to quickly identify adversarial examples, i.e., input values for which the NN prediction exhibits large constraint violations. This hinders the overall solution process. To address this issue, the paper introduces gradient-based attacks that leverage the structure of the OPF problem and of the NN model.

The proposed methodology first identifies data points in the training and test datasets that cause significant constraint violations. These are used as starting points for a projected gradient ascent-based (PGA) local search, wherein gradient steps are applied to iteratively modify the input values (i.e., the active power demand) to increase the constraint violation. The use of multiple starting points improves the quality of the obtained adversarial examples, and makes use of the GPUs' parallelization capability.

The PGA algorithm is applied to the following optimization problem for the power balance violation

$$\max_{\mathbf{p}^d} \mathcal{L}^{\text{PB}} = v^{\text{PB}} \quad (13a)$$

$$\text{s.t. } v^{\text{PB}} = |\mathbf{e}^\top \hat{\mathbf{p}}^g - \mathbf{e}^\top \mathbf{p}^d| \quad (13b)$$

$$(2), (8a) - (8e) \quad (13c)$$

$$\underline{\mathbf{p}}^d \leq \mathbf{p}^d \leq \bar{\mathbf{p}}^d \quad (13d)$$

Each iteration of the PGA algorithm can be formulated as follows:

$$\tilde{\mathbf{p}}_{i+1}^d \leftarrow \tilde{\mathbf{p}}_i^d + \lambda \nabla_{\mathbf{p}^d} \mathcal{L}^{\text{PB}}(\tilde{\mathbf{p}}_i^d) \quad (14a)$$

$$\tilde{\mathbf{p}}_{i+1}^d \leftarrow \min(\max(\tilde{\mathbf{p}}_{i+1}^d, \underline{\mathbf{p}}^d), \bar{\mathbf{p}}^d) \quad (14b)$$

TABLE I
THE CHARACTERISTICS OF TEST CASES.

Test Case	N_b	N_d	N_g	N_l	$\dagger \mathbf{p}^{\max}$
ieee300	300	199	57	411	23525
goc793	793	507	97	913	13198
pegase1k	1354	674	260	1991	121766
pegase2k	2869	1485	510	4582	132437

\dagger Maximum total active load, in MW

where $\tilde{\mathbf{p}}_{i+1}^d$ is the adversarial input after the i th PGA iteration, and λ is the learning rate for the gradient ascent. The initial value $\tilde{\mathbf{p}}_0^d$ is the selected adversarial data point taken from the training set. Similarly, for the worst-case line flow violation, the optimization problem can be formulated as follows:

$$\max_{\mathbf{p}^d} \mathcal{L}^l = v^l \quad (15a)$$

$$\text{s.t. } v^l = \max(0, |\mathbf{p}^f| - \bar{\mathbf{p}}^f) \quad (15b)$$

$$\mathbf{p}^f = \Phi(\hat{\mathbf{p}}^g - \mathbf{p}^d) \quad (15c)$$

$$(2), (8a) - (8e) \quad (15d)$$

$$\underline{\mathbf{p}}^d \leq \mathbf{p}^d \leq \bar{\mathbf{p}}^d \quad (15e)$$

Finally, the PGA algorithm can be implemented directly using backpropagation algorithms for NN training. This allows the local heuristic to be executed on a GPU, enabling fast computations and parallel multi-starts.

IV. NUMERICAL RESULTS

State-of-the-art techniques for extracting worst-case guarantees in power system applications do not scale to large power systems and complex neural networks. This section demonstrates how the proposed acceleration schemes produce dramatic improvements compared to the state-of-the-art in MILP-based NN verification. The results are presented for DC-OPF problems and four different test power systems: the *ieee300*, *goc793*, *pegase1k*, and *pegase2k* systems from the PGLib-OPF network library v19.05 [20]. The test system characteristics are given in Table I. Namely, the table reports, for each system: the number of buses (N_b), loads (N_d), generators (N_g), and branches (N_l), and the maximum total active load in the dataset, in MW.

The training dataset is created by assuming that the demand at each node varies between 60% and 100% of its nominal loading. The sum of the maximum load over all nodes for each system is given in Table I. A dataset of 10,000 random input values were generated for each test case using Latin hypercube sampling [21]. 70% of them were assigned to the training dataset, 10% to the validation set, and 20% to the unseen test dataset. MATPOWER [22] was used to solve the DC-OPF problem and determine the optimal generation set-points. The NN were implemented in PyTorch [23] and used the Adam optimizer [24] for training, with a learning rate of 0.001. WandB [25] was used to monitor and tune the hyperparameters. The MILP-based NN verifiers were solved

TABLE II
AVERAGE NEURAL NETWORK PERFORMANCE

Case	N_k	$\mathcal{L}_0^{\text{test}}$	v_{avg}^{PB}	v_{avg}^l
ieee300	50	0.29	0.23	0.00
goc793	50	0.37	0.27	0.00
pegase1k	50	0.38	0.16	0.18
pegase2k	100	0.42	0.21	0.19

using the Gurobi solver [26]. The NNs were trained on a High-Performance Computing (HPC) server with an Intel Xeon E5-2650v4 processor and 256 GB RAM. The code and datasets to reproduce the results are available online [27].

A. Average Neural Network Performance

The experiments use NNs with three hidden layers with N_k units to predict DC-OPF solutions. All NNs are trained until convergence and use early stopping to prevent overfitting. Table II reports, for each system: the number of nodes in the hidden layers (N_k), the average test loss ($\mathcal{L}_0^{\text{test}}$, in %), the average power balance violations (v_{avg}^{PB} , in %), and the average line flow violation (v_{avg}^l , in %). Recall that the loss function \mathcal{L} is defined in Eq. (7). The relative constraint violations v_{avg}^{PB} and v_{avg}^l are expressed in percentage, relative to the maximum total load and each branch's line flow capacity, respectively.

The results of Table II show that all the NN models are performing adequately well, with less than 0.5 % average prediction error in the test set. Furthermore, all NN have low average constraint violations.

B. The Impact of the Primal Acceleration

Tables III and IV compare the primal bounds available in the training dataset with those found by applying the acceleration technique. The PGA algorithm was applied to the fifty worst inputs in the dataset. The table reports the warm-start primal bounds obtained in the dataset and with the acceleration technique. It also reports the best primal and dual bounds found by the MILP-based NN verifier in 5 hours.

The results show that the PGA acceleration identifies data points with significantly larger worst-case violations than those available in the dataset. In all cases but the *pegase1k* problem, the worst-case violations obtained using PGA were almost twice as large as the worst-case data point from the dataset. Furthermore, in the *ieee300* and *pegase1k* problems, the data points generated by PGA are close to the worst-case constraint violations. In the *goc793* and *pegase2k* problems, the MILP-based NN verification was unable to find significantly better solutions even after 5 hours. On the *ieee300* and *pegase1k* systems, the primal acceleration techniques find near-optimal solutions. In the remaining test cases, it finds primal solutions that are close the best-found primal solutions. The primal acceleration is thus a critical tool for NN verification.

C. The Impact of the Dual Acceleration

This section compares the best dual bound that the Gurobi solver was able to obtain after solving for 5 hours when

TABLE III
WORST-CASE VIOLATIONS OF THE POWER FLOW BALANCE CONSTRAINTS.

Case	Warm-Start Primal Bounds		MILP	
	Dataset	PGA	Primal	Dual
ieee300	6.24	13.64	14.39	14.39
goc793	8.68	28.89	29.71	61.76
pegase1k	24.48	24.67	24.69	24.69
pegase2k	11.91	23.00	23.01	77.75

All values are in % w.r.t the max loading.

TABLE IV
WORST-CASE VIOLATIONS OF THE LINE FLOW CONSTRAINTS.

Case	Warm-Start Primal Bounds		MILP	
	Dataset	PGA	Primal	Dual
ieee300	0.00	0.00	0.00	0.00
goc793	20.87	35.34	36.16	64.27
pegase1k	1.50	1.53	1.54	1.54
pegase2k	17.02	41.64	42.45	123.54

All values are in % w.r.t the line capacity.

TABLE V
WORST CASE POWER FLOW BALANCE

Case	OBBT Technique			MILP
	IBP	MILP	α, β -CROWN	Primal
ieee300	41.33	31.25	14.39	14.39
goc793	86.08	70.70	61.76	29.71
pegase1k	48.27	37.68	24.69	24.69
pegase2k	93.49	86.81	77.75	23.01

All values are in % w.r.t the max loading.

using different optimization-based bounds tightening (OBBT) techniques: Interval Bound Propagation (IBP), the MILP formulation from [7], and α, β -CROWN for getting the RELU big-M bounds. Both α, β -CROWN and the MILP algorithm for finding big-M bounds were run for 10s per ReLU. This is a highly parallelizable task that can be run on multiple GPUs in the case of α, β -CROWN and CPUs in the case of MILPs.

Remarkably, the results show that the proposed methodology converges on the *ieee300* and *pegase1k* systems. This was impossible with the state-of-the-art OBBT techniques like MILP-based OBBT or IBP. Furthermore, in *pegase2k* and *goc793*, the big-M bound given by α, β -CROWN helped significantly close the gap between the primal and dual bounds. This shows the substantial value of α, β -CROWN for NN verification. problem. Similarly, for worst-case line flow constraint violations, the proposed approach converges on the *pegase1k* system, which is out of reach for the state-of-the-art. It also closes the gap between the primal and dual bounds on the *pegase2k* and *goc793* systems. When comparing the computational times for the cases that converged in 5 hours, Table VII shows that α, β -CROWN was able to converge much faster than the other technique.

V. CONCLUSION

This paper proposes two methods to accelerate the exact verification of the NNs for Large-Scale Optimal Power Flow.

TABLE VI
WORST CASE LINE FLOW CONSTRAINT VIOLATION

Case	OBBT Technique			MILP
	IBP	MILP	α, β -CROWN	Primal
ieee300	0.00	0.00	0.00	0.00
goc793	137.42	65.94	64.27	36.16
pegase1k	9.27	4.72	1.54	1.54
pegase2k	162.96	130.85	123.54	42.45

All values are in % w.r.t the line capacity.

TABLE VII
COMPUTING TIME STATISTICS

Case	OBBT technique			
	IBP	MILP	α, β -CROWN	
ieee300	v_{PB}	-	-	7595.00
	v_l	5.79	3.27	1.59
pegase1k	v_{PB}	-	-	147.00
	v_l	7244.02	7234.50	2114.46

All values are in seconds. In case of v_{PB} both for *ieee300* and *pegase1k* system only the MILP-based verification that used α, β -CROWN for OBBT managed to converge.

Firstly, we propose a gradient-based method for finding adversarial test cases for OPF proxies that can find test cases that are close to the worst-case constraint violations. Secondly, we show the benefits of using advanced bound-tightening techniques, in particular α, β -CROWN, to tighten the MIP dual bounds. The proposed methodology converges on the *ieee300* and *pegase1k* systems, which was impossible with the state-of-the-art OBBT techniques. This is significant, as it makes it possible to use formal verification to ensure the safety and reliability of power grids. In the future, more effective cutting planes will be explored to narrow the gap between primal and dual bounds.

REFERENCES

- [1] J. Carpentier, "Optimal power flows," *International Journal of Electrical Power & Energy Systems*, vol. 1, no. 1, pp. 3–15, 1979.
- [2] D. Deka and S. Misra, "Learning for dc-opf: Classifying active sets using neural nets," in *2019 IEEE Milan PowerTech*, 2019, pp. 1–6.
- [3] O. A. Alimi, K. Ouahada, and A. M. Abu-Mahfouz, "A review of machine learning approaches to power system security and stability," *IEEE Access*, vol. 8, pp. 113 512–113 531, 2020.
- [4] F. Hasan, A. Kargarian, and A. Mohammadi, "A survey on applications of machine learning for optimal power flow," in *2020 IEEE Texas Power and Energy Conference (TPEC)*, 2020, pp. 1–6.
- [5] L. Duchesne, E. Karangelos, and L. Wehenkel, "Recent developments in machine learning for energy systems reliability management," *Proceedings of the IEEE*, vol. 108, no. 9, pp. 1656–1676, 2020.
- [6] A. Kody, S. Chevalier, S. Chatzivasileiadis, and D. Molzahn, "Modeling the ac power flow equations with optimally compact neural networks: Application to unit commitment," *Electric Power Systems Research*, vol. 213, p. 108282, 2022.
- [7] A. Venzke, G. Qu, S. Low, and S. Chatzivasileiadis, "Learning optimal power flow: Worst-case guarantees for neural networks," in *2020 IEEE International Conference on Communications, Control, and Computing Technologies for Smart Grids (SmartGridComm)*. IEEE, 2020, pp. 1–7.
- [8] R. Nellikkath and S. Chatzivasileiadis, "Physics-Informed Neural Networks for Minimising Worst-Case Violations in DC Optimal Power Flow," in *2021 IEEE International Conference on Communications, Control, and Computing Technologies for Smart Grids (SmartGridComm)*, 2021, pp. 419–424.

- [9] —, “Physics-Informed Neural Networks for AC Optimal Power Flow,” *Electric Power Systems Research*, vol. 212, p. 108412, 2022. [Online]. Available: <https://www.sciencedirect.com/science/article/pii/S0378779622005636>
- [10] S. Chevalier and S. Chatzivasileiadis, “Global performance guarantees for neural network models of ac power flow,” *arXiv preprint arXiv:2211.07125*, 2022.
- [11] R. Nellikkath and S. Chatzivasileiadis, “Minimizing worst-case violations of neural networks,” *arXiv preprint arXiv:2212.10930*, 2022.
- [12] —, “Enriching neural network training dataset to improve worst-case performance guarantees,” *arXiv preprint arXiv:2303.13228*, 2023.
- [13] K. Xu, H. Zhang, S. Wang, Y. Wang, S. Jana, X. Lin, and C.-J. Hsieh, “Fast and Complete: Enabling complete neural network verification with rapid and massively parallel incomplete verifiers,” in *International Conference on Learning Representations*, 2021. [Online]. Available: <https://openreview.net/forum?id=nVZtXB16LNn>
- [14] H. Zhang, T.-W. Weng, P.-Y. Chen, C.-J. Hsieh, and L. Daniel, “Efficient neural network robustness certification with general activation functions,” *Advances in Neural Information Processing Systems*, vol. 31, pp. 4939–4948, 2018. [Online]. Available: <https://arxiv.org/pdf/1811.00866.pdf>
- [15] S. Wang, H. Zhang, K. Xu, X. Lin, S. Jana, C.-J. Hsieh, and J. Z. Kolter, “Beta-CROWN: Efficient bound propagation with per-neuron split constraints for complete and incomplete neural network verification,” *Advances in Neural Information Processing Systems*, vol. 34, 2021.
- [16] S. Chevalier, I. Murzakanov, and S. Chatzivasileiadis, “Gpu-accelerated verification of machine learning models for power systems,” 2023.
- [17] B. Stott, J. Jardim, and O. Alsac, “Dc power flow revisited,” *IEEE Transactions on Power Systems*, vol. 24, no. 3, pp. 1290–1300, 2009.
- [18] R. Anderson, J. Huchette, W. Ma, C. Tjandraatmadja, and J. P. Vielma, “Strong mixed-integer programming formulations for trained neural networks,” *Mathematical Programming*, vol. 183, no. 1-2, pp. 3–39, 2020.
- [19] M. N. Müller, C. Brix, S. Bak, C. Liu, and T. T. Johnson, “The third international verification of neural networks competition (vnn-comp 2022): summary and results,” *arXiv preprint arXiv:2212.10376*, 2022.
- [20] S. Babaeinejadsarookolae, A. Birchfield, R. D. Christie, C. Coffrin, C. DeMarco, R. Diao, M. Ferris, S. Fliscounakis, S. Greene, R. Huang *et al.*, “The power grid library for benchmarking ac optimal power flow algorithms,” *arXiv preprint arXiv:1908.02788*, 2019.
- [21] M. D. McKay, R. J. Beckman, and W. J. Conover, “A comparison of three methods for selecting values of input variables in the analysis of output from a computer code,” *Technometrics*, vol. 42, no. 1, pp. 55–61, 2000.
- [22] R. D. Zimmerman, C. E. Murillo-Sánchez, and R. J. Thomas, “Matpower: Steady-state operations, planning, and analysis tools for power systems research and education,” *IEEE Transactions on power systems*, vol. 26, no. 1, pp. 12–19, 2010.
- [23] A. Paszke, S. Gross, F. Massa, A. Lerer, J. Bradbury, G. Chanan, T. Killeen, Z. Lin, N. Gimelshein, L. Antiga, A. Desmaison, A. Kopf, E. Yang, Z. DeVito, M. Raison, A. Tejani, S. Chilamkurthy, B. Steiner, L. Fang, J. Bai, and S. Chintala, “Pytorch: An imperative style, high-performance deep learning library,” in *Advances in Neural Information Processing Systems 32*, H. Wallach, H. Larochelle, A. Beygelzimer, F. d’Alché-Buc, E. Fox, and R. Garnett, Eds. Curran Associates, Inc., 2019, pp. 8024–8035. [Online]. Available: <http://papers.neurips.cc/paper/9015-pytorch-an-imperative-style-high-performance-deep-learning-library.pdf>
- [24] D. P. Kingma and J. Ba, “Adam: A method for stochastic optimization,” in *3rd International Conference on Learning Representations, ICLR 2015, San Diego, CA, USA, May 7-9, 2015, Conference Track Proceedings*, Y. Bengio and Y. LeCun, Eds., 2015. [Online]. Available: <http://arxiv.org/abs/1412.6980>
- [25] L. Biewald, “Experiment tracking with weights and biases,” 2020, software available from wandb.com. [Online]. Available: <https://www.wandb.com/>
- [26] Gurobi Optimization, LLC, “Gurobi Optimizer Reference Manual,” 2022. [Online]. Available: <https://www.gurobi.com>
- [27] P. V. H. R. Nellikkath, M. Tanneau and S. Chatzivasileiadis, “Supplementary data and code: Scalable exact verification of optimization proxies for large-scale optimal power flow,” 2023. [Online]. Available: <https://github.com/RahulNellikkath/ScalableExactVerification>